JACS
JOURNAL OF THE AMERICAN CHEMICAL SOCIETY
Article
pubs.acs.org/JACS

Synthesis, Characterization, and Stoichiometric U−O Bond Scission in Uranyl Species Supported by Pyridine(diimine) Ligand Radicals

John J. Kiernicki,[†] Dennis P. Cladis,[†] Phillip E. Fanwick,[†] Matthias Zeller,[‡] and Suzanne C. Bart*[,†]

[†]H.C. Brown Laboratory, Department of Chemistry, Purdue University, West Lafayette, Indiana 47906, United States
[‡]Department of Chemistry, Youngstown State University, Youngstown, Ohio 44555, United States

Supporting Information

ABSTRACT: Two uranium(VI) uranyl compounds, Cp*UO_2($^{Mes}PDI^{Me}$) (**3**) and Cp*UO_2(^{t}Bu-$^{Mes}PDI^{Me}$) (**3-^{t}Bu**) (Cp* = 1,2,3,4,5-pentamethylcyclopentadienide; $^{Mes}PDI^{Me}$ = 2,6-((Mes)N=CMe)$_2C_5H_3N$; ^{t}Bu-$^{Mes}PDI^{Me}$ = 2,6-((Mes)-N=CMe)$_2$-*p*-C(CH_3)$_3C_5H_2N$; Mes = 2,4,6-trimethylphenyl), have been synthesized by addition of *N*-methylmorpholine *N*-oxide to trianionic pyridine(diimine) uranium(IV) precursors, Cp*U($^{Mes}PDI^{Me}$)(THF) (**1**), Cp*U($^{Mes}PDI^{Me}$)(HMPA) (**1-HMPA**), and Cp*U(^{t}Bu-$^{Mes}PDI^{Me}$)(THF) (**1-^{t}Bu**). These uranyl complexes contain singly reduced pyridine(diimine) ligands suggesting formation occurs via cooperative ligand/metal oxidation. Treating **3** or **3-^{t}Bu** with stoichiometric equivalents of Me_3SiI results in stepwise oxo silylation to form (Me_3SiO)$_2UI_2$($^{Mes}PDI^{Me}$) (**5**) or (Me_3SiO)UI_2(^{t}Bu-$^{Mes}PDI^{Me}$) (**5-^{t}Bu**), respectively. Additional equivalents result in full uranium−oxo bond scission and formation of UI_4(1,4-dioxane)$_2$ with extrusion of hexamethyldisiloxane. The uranium complexes have been characterized via multinuclear NMR, vibrational, and electronic absorption spectroscopies and, in some cases, X-ray crystallography.

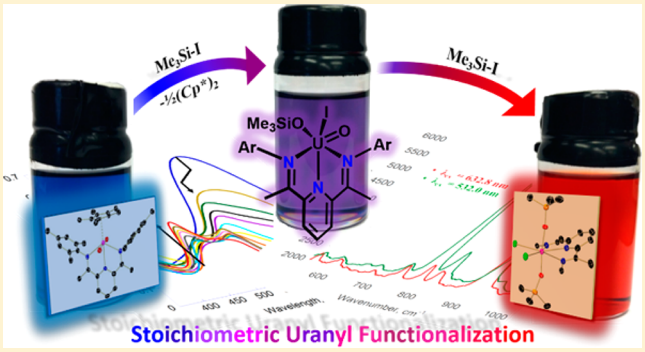

INTRODUCTION

The reduction of the strong uranium−oxygen multiple bonds in the uranyl dication, $[UO_2]^{2+}$, has been studied using a variety of strategies, including chemical, microbial, thermal, and photoprocesses.[1] Such transformations have important applications, including environmental remediation[2] and nuclear fuels processing.[3,4] One such pathway popularized recently is reductive silylation,[5] which takes advantage of a strong thermodynamic driving force for the formation of Si−O bonds for activation of the robust uranium−oxygen multiple bonds. Pioneering work by Ephritikhine demonstrated full uranyl U−O bond cleavage via reductive silylation by addition of a large excess of Me_3Si−X (X = Cl, Br, I) to $UO_2I_2(THF)_3$ generating $UX_4(NCMe)_4$.[6] This proved to be an effective strategy for the generation of uranium halide starting materials, but using an excess of silylating reagent is problematic for homogeneous systems with alkoxide ligands, as the U−O silylation is not selective.[7] Following this, Arnold showed controlled silylation of a uranyl using a polypyrrolic Pacman ligand system, which serves to activate one end of the uranyl unit for functionalization to occur at the other.[5,8,9] More recently, Hayton extended reductive silylation chemistry to silanes, showing U−O silylation could be achieved in the presence of a Lewis acid, which activates the Si−H bond.[10−12]

Uranyl reduction is generally thought to proceed through the pentavalent uranyl ion, $[UO_2]^{+}$.[13] However, these complexes can be difficult to isolate due to the propensity for uranium(V) complexes to disproportionate to uranium(IV) and uranium(VI) products.[14] While pentavalent uranyl complexes have been successfully isolated,[15] they are relatively rare as compared to their higher valent counterparts. One synthetic strategy for pentavalent uranyl formation not commonly attempted is the use of redox noninnocent ligands, which are routinely used to generate masked forms of lower valent metal species. Recently, Ikeda demonstrated this principle with the formation of $[UO_2$(gha)(dmso)$]^{-}$ (gha = glyoxal bis(2-hydroxanil)ate; dmso = dimethyl sulfoxide).[16] While formally this would appear as a pentavalent uranyl anion, this molecule is more accurately described with a hexavalent uranium center supported by a radical glyoxal ligand. This was confirmed using spectroelectrochemistry and further probed using DFT calculations. Due to the transient nature of $[UO_2$(gha)-DMSO$]^{-}$, neither ^{1}H NMR spectroscopic nor X-ray crystallographic analyses were possible.

Recently, we have shown the redox noninnocent pyridine(diimine) ligand, $^{Mes}PDI^{Me}$, can also support ligand radicals at low-valent uranium.[17] For instance, characterization of Cp*U($^{Mes}PDI^{Me}$)(THF) by X-ray crystallography elucidated ligand distortions that were consistent with a trianionic ligand, $[^{Mes}PDI^{Me}]^{3-}$, thus formulating the uranium center to be in the +4 oxidation state rather than the +1 oxidation state that

Received: June 15, 2015
Published: August 24, 2015

ACS Publications © 2015 American Chemical Society

DOI: 10.1021/jacs.5b06217
J. Am. Chem. Soc. 2015, 137, 11115−11125

Table 1. Structural Parameters of 1-^{t}Bu, 1-HMPA, 3, 3-^{t}Bu, and 5

bond (Å) or angle (deg)	1-^{t}Bu[a,d]	1-HMPA[b,d]	3[a,e]	3-^{t}Bu[c,e]	5[a,d]
U1−O1	2.540(3)	2.339(2)	1.799(5)	1.766(10)	2.091(10)
U1−O2			1.790(5)		2.098(10)
U1−I1					3.0992(9)
U1−Ct	2.553	2.539	2.582	2.588	
U1−N1	2.293(2)	2.338(3)	2.529(6)	2.417(8)	2.737(9)
U1−N2	2.204(3)	2.234(3)	2.547(6)	2.548(9)	2.605(13)
U1−N3		2.333(3)	2.504(6)	2.603(9)	
N1−C2	1.418(4)	1.426(4)	1.308(11)	1.306(15)	1.246(13)
C2−C3	1.372(4)	1.361(5)	1.424(11)	1.477(15)	1.503(16)
C3−C4	1.489(4)	1.477(5)	1.487(11)	1.408(16)	1.403(17)
C4−C5	1.429(3)	1.415(6)	1.416(12)	1.391(16)	1.382(15)
C5−C6		1.403(5)	1.384(12)	1.373(15)	
C6−C7		1.481(5)	1.471(11)	1.380(16)	
C7−C8		1.371(5)	1.421(11)	1.487(15)	
N2−C3	1.407(3)	1.399(4)	1.339(10)	1.350(13)	1.354(13)
N2−C7		1.388(5)	1.354(10)	1.380(13)	
N3−C8		1.421(5)	1.308(10)	1.270(15)	
O1−U1−O2			168.3(2)	167.4(4)	172.3(4)

[a] T = 150 K. [b] T = 100 K. [c] T = 200 K. [d] λ = 0.71073 Å. [e] λ = 1.54184 Å.

would accompany a neutral ligand.[18] Interestingly, this reduced ligand serves as a potent reductant toward strong bonds, specifically the N═N double bond in azobenzene, completely cleaving this bond and generating the uranium *trans*-bis(imido) species, Cp*U(NPh)$_2$(^{Mes}PDI^{Me}). In this case, all three electrons from the ligand framework plus one from the uranium center were used to perform this four-electron cleavage, leaving a neutral ^{Mes}PDI^{Me} ligand supporting a U(V) species. Noting that ligand oxidation was facile in this case, we hypothesized the analogous pentavalent uranyl species could be formed from Cp*U(^{Mes}PDI^{Me})(THF) using an oxo transfer agent. Surprisingly, a hexavalent uranyl species supported by a ^{Mes}PDI^{Me} radical was the preferred resonance form by analogy to [UO$_2$(gha)DMSO]$^-$. Herein, we report the synthesis, isolation, and full characterization of this unusual uranyl species along with its unprecedented stoichiometric reductive silylation chemistry using Me$_3$SiI, which results in U−O bond scission.

EXPERIMENTAL SECTION

All air- and moisture-sensitive manipulations were performed using standard Schlenk techniques or in an MBraun inert atmosphere drybox with an atmosphere of purified nitrogen. The MBraun drybox was equipped with a cold well designed for freezing samples in liquid nitrogen as well as two −35 °C freezers for cooling samples and crystallizations. Solvents for sensitive manipulations were dried and deoxygenated using literature procedures with a Seca solvent purification system.[19] Benzene-d_6 was purchased from Cambridge Isotope Laboratories, dried with molecular sieves and sodium, and degassed by three freeze−pump−thaw cycles. 4-*tert*-Butyl-2,6-diacetylpyridine,[25] Cp*$_2$UI(THF),[20] potassium graphite,[21] Cp*U(^{Mes}PDI^{Me})(THF),[18] and UI$_4$(dioxane)$_2$[22] were prepared according to literature procedures. *N*-Methylmorpholine *N*-oxide, iodotrimethylsilane, and potassium trimethylsilanolate were purchased from Sigma-Aldrich and used as received, whereas hexamethylphosphoric triamide was distilled from CaH$_2$ prior to use.

^{1}H NMR spectra were recorded on a Varian Inova 300 spectrometer operating at 299.992 MHz. All chemical shifts are reported relative to the peak for SiMe$_4$ using ^{1}H (residual) chemical shifts of the solvent as a secondary standard. The spectra for paramagnetic molecules were obtained by using an acquisition time of 0.5 s; thus, the peak widths reported have an error of ±2 Hz. For paramagnetic molecules, the ^{1}H NMR data are reported with the chemical shift, followed by the peak width at half height in Hertz, the integration value, and, where possible, the peak assignment. ^{31}P spectra were recorded on a Varian Inova 300 spectrometer operating at 121.423 MHz, and chemical shifts are reported relative to 85% H$_3$PO$_4$. Elemental analyses were performed by Complete Analysis Laboratories, Inc., Parsippany, NJ. Electronic absorption measurements were recorded at 294 K in sealed 1 cm quartz cuvettes with a Jasco V-6700 spectrophotometer.

Single crystals suitable for X-ray diffraction were coated with poly(isobutylene) oil in a glovebox and quickly transferred to the goniometer head of the specified instrument. Crystals of Cp*U(^{t}Bu-^{Mes}PDI^{Me})(THF) (**1-^{t}Bu**), Cp*UO$_2$(^{Mes}PDI^{Me}) (**3**), and (Me$_3$SiO)$_2$UI$_2$(^{Mes}PDI^{Me}) (**5**) were transferred to the goniometer head of a Nonius KappaCCD image plate diffractometer equipped with a graphite crystal and incident beam monochromator and examined with Mo Kα radiation (λ = 0.71073 Å). Crystals of Cp*UO$_2$(^{Mes}PDI^{Me}) (**3**) and Cp*UO$_2$(^{t}Bu-^{Mes}PDI^{Me}) (**3-^{t}Bu**) were transferred to the goniometer head of a Rigaku Rapid II image plate diffractometer equipped with a MicroMax002+ high-intensity copper X-ray source with confocal optics and examined with Cu Kα radiation (λ = 1.54184 Å). Crystals of Cp*U(^{Mes}PDI^{Me})(HMPA) (**1-HMPA**) were transferred to a Bruker AXS D8 Quest CMOS diffractometer equipped with a complementary metal−oxide−semiconductor (CMOS) detector and I-μ-S Mo Kα microsource X-ray tube (λ = 0.71073 Å) operated at 50 kV and 1 mA with laterally graded multilayer (Goebel) mirror X-ray optics. Data were collected at low temperature (see Table 1).

Synthesis of Cp*U(^{t}Bu-^{Mes}PDI^{Me})(THF) (1-^{t}Bu). A 20 mL scintillation vial was charged with Cp*$_2$UI(THF) (0.200 g, 0.282 mmol), ^{t}Bu-^{Mes}PDI^{Me} (0.129 g, 0.284 mmol), and 10 mL of toluene and stirred for 30 min resulting in a color change from green to brown. Potassium graphite (0.115 g, 0.851 mmol) was then added to the mixture and stirred an additional 2 h. After removal of volatiles in vacuo, the product was extracted into diethyl ether, filtered over Celite, and subsequently dried to afford brown powder (0.242 g, 0.269 mmol, 95%) assigned as Cp*U(^{t}Bu-^{Mes}PDI^{Me})(THF). Single, X-ray-quality crystals were obtained from a concentrated diethyl ether solution at −35 °C. Anal. Calcd for C$_{45}$H$_{62}$N$_3$OU: C, 60.12; H, 6.95; N, 4.67. Found: C, 59.85; H, 6.89; N, 4.78. ^{1}H NMR (C$_6$D$_6$, 25 °C): δ = −34.14 (42, 2H, 2-THF−CH_2), −33.49 (41, 2H, 2-THF−CH_2), −15.16 (40, 2H, 3-THF−CH_2), −15.06 (41, 2H, 3-THF−CH_2), −3.78 (3, 9H, C(CH_3)$_3$), −2.55 (3, 15H, Cp*−CH_3), 2.01 (3, 3H, *p*-Ar−CH_3), 2.40 (3, 3H, *p*-Ar−CH_3), 7.45 (d, J = 18, 1H, *m*-pyr−CH), 8.70 (6, 1H, *m*-Ar−CH), 9.04 (4, 1H, *m*-Ar−CH), 10.00 (5, 1H, *m*-

DOI: 10.1021/jacs.5b06217
J. Am. Chem. Soc. 2015, 137, 11115−11125

Ar−C*H*), 10.60 (4, 3H, *o*-Ar−CH_3), 12.11 (4, 3H, *o*-Ar−CH_3), 12.84 (4, 3H, *o*-Ar−CH_3), 13.16 (5, 1H, *m*-Ar−C*H*), 13.70 (4, 3H, *o*-Ar−CH_3), 24.02 (4, 3H, N=CCH_3), 24.50 (d, *J* = 23, 1H, *m*-pyr−C*H*), 27.36 (4, 3H, N=CCH_3).

Synthesis of Cp*UO_2(^{Mes}PDI^{Me}) (3). A 20 mL scintillation vial was charged with Cp*U(^{Mes}PDI^{Me})(THF) (**1**) (0.110 g, 0.130 mmol) and 5 mL of toluene. To this, *N*-methylmorpholine *N*-oxide (0.031 g, 0.265 mmol) was added as a solid and the solution stirred for 3 h, resulting in a gradual color change from brown to dark blue. Volatiles were removed in vacuo, and the product was extracted into *n*-hexane. The solution was dried, affording blue powder (0.087 g, 0.108 mmol, 83%) assigned as Cp*UO_2(^{Mes}PDI^{Me}). Single, X-ray-quality crystals were obtained from either concentrated pentane/THF (10:1) or ether/pentane/toluene (10:2:1) solutions at −35 °C. Anal. Calcd for $C_{37}H_{46}N_3O_2U$: C, 55.36; H, 5.78; N, 5.23. Found: C, 55.44; H, 5.85; N, 5.18. ^{1}H NMR (C_6D_6, 25 °C): δ = 1.18 (s, 3H, N=CCH_3), 1.42 (s, 3H, N=CCH_3), 2.22 (s, 6H, Ar−CH_3), 2.24 (s, 6H, Ar−CH_3), 2.27 (s, 6H, Ar−CH_3), 3.63 (d, *J* = 3.9, 1H, *m*-pyr−C*H*), 4.50 (s, 15H, Cp*), 5.02 (dt, *J* = 3.9, 9.9, 1H, *p*-pyr−C*H*), 6.18 (d, *J* = 9.9, 1H, *m*-pyr−C*H*), 6.89 (s, 2H, Ar−C*H*), 6.90 (s, 2H, Ar−C*H*). ^{13}C NMR (C_6D_6, 25 °C): δ = 6.99 (q, *J* = 19, Cp*−CH_3), 17.71 (q, *J* = 16, N=CCH_3), 18.12 (Ar−CH_3), 18.33 (N=CCH_3), 18.64 (Ar−CH_3), 18.70 (Ar−CH_3) 29.01 (*m*-pyr−CH), 114.94 (d, *J* = 27, *m*-pyr−CH), 129.56 (ArC), 129.51 (d, *J* = 33, Ar−CH), 129.61 (d, *J* = 34, Ar−CH), 132.42 (ArC), 133.55 (ArC), 135.21 (ArC), 135.51 (ArC), 137.37 (Cp*−CCH_3), 145.46 (ArC), 145.68 (ArC), 167.33 (ArC), 172.69 (ArC). IR: $\upsilon_{(O=U=O\ asym)}$ = 876 cm^{-1}. rRaman: $\upsilon_{(O=U=O\ sym)}$ = 788 cm^{-1}. UV−vis (λ_{max}, ε): 285 (16 542 M^{-1} cm^{-1}), 344 (10 694 M^{-1} cm^{-1}), 611 nm (11 439 M^{-1} cm^{-1}).

Synthesis of Cp*UO_2(^{t}Bu-^{Mes}PDI^{Me}) (3-^{t}Bu). A 20 mL scintillation vial was charged with Cp*U(^{t}Bu-^{Mes}PDI^{Me})(THF) (**1-^{t}Bu**) (0.200 g, 0.222 mmol) and 5 mL of toluene. To this, *N*-methylmorpholine *N*-oxide (0.052 g, 0.444 mmol) was added as a solid, and the solution was stirred for 10 min resulting in a fast color change from brown to dark blue. Volatiles were removed in vacuo, and the product was extracted into *n*-pentane. The solution was dried, affording blue powder (0.165 g, 0.192 mmol, 86%) assigned as Cp*UO_2(^{t}Bu-^{Mes}PDI^{Me}). Single, X-ray-quality crystals were obtained from a concentrated pentane/THF (20:1) solution at −35 °C. Anal. Calcd for $C_{41}H_{54}N_3O_2U$: C, 57.33; H, 6.34; N, 4.89. Found: C, 57.22; H, 6.40; N, 4.84. ^{1}H NMR (C_6D_6, 25 °C): δ = 1.01 (s, 9H, C(CH_3)$_3$) 1.44 (s, 3H, N=CCH_3), 1.63 (s, 3H, N=CCH_3), 2.10 (s, 6H, Ar−CH_3), 2.27 (s, 6H, Ar−CH_3), 2.31 (s, 6H, Ar−CH_3), 3.76 (s, 1H, *m*-pyr−C*H*), 4.51 (s, 15H, Cp*), 6.21 (s, 1H, *m*-pyr−Ar*H*), 6.92 (s, 2H × 2, overlapping Ar−C*H*). ^{13}C NMR (C_6D_6, 25 °C): δ = 7.61 (q, *J* = 18.6, Cp*−CH_3), 14.83 (Ar−CH_3), 18.22 (q, *J* = 15.6, N=C−CH_3), 18.70 (q, *J* = 21.6, N=C−CH_3), 19.19 (Ar−CH_3), 23.26 (C(CH_3)$_3$), 28.49 (C(CH_3)$_3$), 28.83 (*m*-pyr−CH), 35.42 (Ar−CH), 114.45 (*m*-pyr−CH), 129.91 (ArC), 130.24 (d, *J* = 27.6, Ar−CH), 130.36 (d, *J* = 23.1, Ar−CH), 133.02 (ArC), 133.78 (ArC), 135.58 (ArC), 135.76 (ArC), 136.21 (ArC), 137.77 (Cp*−CCH_3), 145.93 (ArC), 168.27 (ArC), 172.07 (ArC). IR: $\upsilon_{(O=U=O\ asym)}$ = 878 cm^{-1}; $\upsilon_{(O=U=O\ sym)}$ = 787 cm^{-1}. UV−vis (λ_{max}, ε): 284 (13 435 M^{-1} cm^{-1}), 346 (7143 M^{-1} cm^{-1}), 620 nm (7455 M^{-1} cm^{-1}).

Synthesis of [$(CH_3)_3SiO$]U(O)I(^{Mes}PDI^{Me}) (4). A 20 mL scintillation vial was charged with Cp*UO_2(^{Mes}PDI^{Me}) (**3**) (0.100 g, 0.125 mmol) and 3 mL of toluene and cooled to −35 °C. Me_3SiI (0.017 mL, 0.119 mmol) was added via microsyringe and cooled again. After 24 h of cold storage, a color change from blue to purple was noted, and the solution was layered with 10 mL of pentane. After cooling for another 24 h, the mother liquor was decanted; the solid was washed with cold pentane and dried to afford dark purple solid (0.031 g, 0.036 mmol, 29%) assigned as [$(CH_3)_3SiO$]U(O)I-(^{Mes}PDI^{Me}). UV−vis: λ_{max} = 575 nm.

Synthesis of [$(CH_3)_3SiO$]$_2UI_2$(^{Mes}PDI^{Me}) (5). A 20 mL scintillation vial was charged with Cp*UO_2(^{Mes}PDI^{Me}) (**3**) (0.140 g, 0.174 mmol) and 5 mL of toluene. Me_3SiI (0.049 mL, 0.344 mmol) was added via microsyringe and stirred for 24 h, resulting in a color change from blue to purple (2−4 h) and finally to red (8−12 h). The solution was then layered with an equal volume of pentane and stored overnight at −35 °C, resulting in precipitation of solid. The mother liquor was decanted and set aside. The solid was dried in vacuo to afford red powder (0.122 g, 0.114 mmol, 66%) assigned as [$(CH_3)_3SiO$]$_2UI_2$(^{Mes}PDI^{Me}). Single, X-ray-quality crystals were obtained from a dilute benzene solution at room temperature. Anal. Calcd for $C_{33}H_{49}N_3O_2Si_2I_2U$: C, 37.12; H, 4.63; N, 3.94. Found: C, 37.13; H, 4.72; N, 3.83. ^{1}H NMR (C_6D_6, 25 °C): δ = −9.26 (47, 12H, *o*-Ar−CH_3), −0.10 (860, 6H, CH_3), 6.25 (37, 6H, CH_3), 11.21 (36, 18H, Si(CH_3)$_3$), 11.65 (29, 4H, *m*-Ar*H*), 15.05 (14, 2H, 3,5-pyr−Ar*H*), 20.31 (4, 1H, 4-pyr−Ar*H*). IR: $\upsilon_{(SiCH3\ symm\ bend)}$ = 1246 cm^{-1}; $\upsilon_{(SiCH3\ asymm\ bend)}$ = 840 cm^{-1}. UV−vis (λ_{max}, ε): 370 (7171 M^{-1} cm^{-1}), 485 nm (11 471 M^{-1} cm^{-1}). The solvent of the mother liquor was evaporated to afford a slurry from which $(C_5Me_5)_2$ was identified by ^{1}H NMR spectroscopy.[24,25]

Synthesis of [$(CH_3)_3SiO$]UI_3(THF)$_3$ (6-THF) from 3. A 20 mL scintillation vial was charged with Cp*UO_2(^{Mes}PDI^{Me}) (**3**) (0.138 g, 0.172 mmol) and 5 mL of toluene. Me_3SiI (0.073 mL, 0.513 mmol) was added via microsyringe and stirred for 48 h, resulting in a color change from blue to purple (0−1 h) and finally to red (4−6 h). Volatiles were removed in vacuo. The resulting solid was washed with pentane and dried to afford a red powder. The red powder was recrystallized from a concentrated THF solution layered with *n*-pentane to afford green/brown powder (0.098 g, 0.106 mmol, 62%) assigned as [$(CH_3)_3SiO$]UI_3(THF)$_3$. ^{1}H NMR (C_6D_6, 25 °C): δ = −6.18 (321, 24H, THF), 50.74 (39, 9H, Si(CH_3)$_3$).

Synthesis of [$(CH_3)_3SiO$]UI_3(Et_2O)$_3$ (6-Et_2O). A 20 mL scintillation vial was charged with UI_4(*p*-dioxane)$_2$ (0.200 g, 0.216 mmol) and 10 mL of diethyl ether and cooled to −35 °C. While stirring, potassium trimethylsilanolate (0.028 g, 0.218 mmol) was added as a solid, resulting in a color change from orange to greenish-brown. Following 30 min of stirring, volatiles were removed in vacuo. The crude mixture was redissolved in THF and filtered over Celite. The solution was concentrated, layered with pentane, and cooled to −35 °C overnight, resulting in the deposition of green crystals (0.080 g, 0.086 mmol, 40%) assigned as [$(CH_3)_3SiO$]UI_3(Et_2O)$_3$. Anal. Calcd for $C_{15}H_{39}O_4Si_1I_3U$: C, 19.37; H, 4.23; N, 0.00. Found: C, 19.07; H, 4.49; N, 0.16. ^{1}H NMR (C_6D_6, 25 °C): δ = −14.33 (523, 12H, Et_2O−CH_2), −9.08 (203, 18H, Et_2O−CH_3), 51.68 (29, 9H, Si(CH_3)$_3$). IR: $\upsilon_{(SiCH\ symm\ bend)}$ = 1249 cm^{-1}; $\upsilon_{(SiCH\ asymm\ bend)}$ = 843 cm^{-1}. UV−vis (λ_{max}, ε): 345 nm (1596 M^{-1} cm^{-1}).

Synthesis of UI_4(L)$_2$ (L = Et_2O, 1,4-dioxane) from (Me_3SiO)-UI_3(Et_2O)$_3$ (L = 1,4-dioxane). A 20 mL scintillation vial was charged with (Me_3SiO)UI_3(Et_2O)$_3$ (0.058 g, 0.062 mmol) and 2 mL of 1,4-dioxane. While stirring, Me_3SiI was added via microsyringe, resulting in an immediate color change to red/orange from translucent yellow/orange. After 5 min, volatiles were removed in vacuo. The resulting solid was washed with *n*-pentane and dried to afford orange solid (0.050 g, 0.054 mmol, 87%) identified by ^{1}H NMR spectroscopy as UI_4(1,4-dioxane)$_2$.[22] For L = Et_2O, a J-Young NMR tube was charged with (Me_3SiO)UI_3(Et_2O)$_3$ (0.018 g, 0.019 mmol), C_6D_6 (0.75 mL), diethyl ether (0.20 mL), and Me_3SiI (via microsyringe, 0.0028 mL, 0.020 mmol). Shaking the tube resulted in an immediate color change to dark red/orange from translucent yellow/orange. ^{1}H NMR spectroscopy revealed the formation of both hexamethyldisiloxane and UI_4(OEt_2)$_2$.[26]

RESULTS AND DISCUSSION

Synthesis and Characterization of Uranyl Complexes. Initial experiments were aimed at the synthesis of the pentavalent uranyl analogue of the previously synthesized bis(imido) species, Cp*U(NPh)$_2$(^{Mes}PDI^{Me}). Treating a toluene solution of Cp*U(^{Mes}PDI^{Me})(THF) (**1**) with 2 equiv of *N*-methylmorpholine *N*-oxide (NMMO) gave an intensely colored blue solid, **3**, after workup (eq 1). Analysis by ^{1}H NMR spectroscopy (benzene-d_6) revealed a C_s-symmetric spectrum featuring 11 resonances ranging from 1.18 to 6.90 ppm, with the largest resonance at 4.50 ppm assignable to the η^5-Cp* ligand. Three singlets (6H) were observed for the mesityl−CH_3 groups as well as two singlets (3H) for the imine −N=CCH_3.

DOI: 10.1021/jacs.5b06217
J. Am. Chem. Soc. 2015, 137, 11115−11125

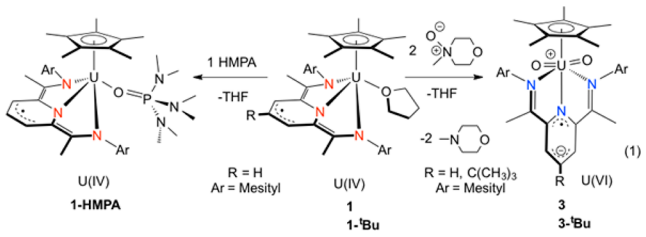

Two pairs of doublets (3.63, 6.18 ppm) for the pyr−C*H* and one doublet of triplets (5.02 ppm) for the *p*-pyr−C*H* confirm asymmetry in the pyridine(diimine) ligand (Figure 1).

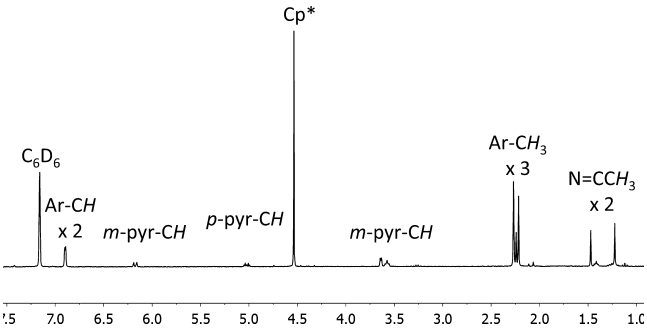

Figure 1. ^{1}H NMR spectrum (C_6D_6, 25 °C) of Cp*UO_2(^{Mes}PDI^{Me}) (**3**).

Due to the asymmetry in the ^{1}H NMR spectrum and unusual blue color of **3**, additional experiments were conducted to confirm its identity. Performing the same experiment with 1 equiv of NMMO resulted in formation of 0.5 equiv of **3** with an equimolar amount of unreacted Cp*U(^{Mes}PDI^{Me})(THF), suggesting two oxygen atoms were transferred to the same uranium during the course of the reaction. Thus, the blue product was assigned as the uranium dioxo product, Cp*UO_2(^{Mes}PDI^{Me}) (**3**). The resonance for the Cp* ligand in **3** has a similar chemical shift to that reported by Ephritikhine and co-workers for the only other cyclopentadienyl uranyl species, [Et_4N]$_2$[Cp*$UO_2(CN)_3$] (4.36 ppm),[27] indicating **3** could be hexavalent. Further, 2D ^{1}H NMR spectroscopic experiments were performed to confirm the assigned connectivity and to corroborate that no protons were overlooked in the analysis (Figure S15). All three pyridine protons display strong coupling to one another. Additionally, each set (3 × 6H) of mesityl methyl resonances couples to the adjacent aryl−C*H*. A HETCOR analysis of **3** revealed surprising chemical shifts of the inequivalent meta pyridine carbons at 114.94 and 29.01 ppm. The large shift from its diamagnetic reference values (^{13}C = 122.44, ^{1}H = 8.54 ppm) for the meta pyridine sp^2-CH (^{13}C = 29.01, ^{1}H = 3.63 ppm) (C6 crystallographically, vide infra) is likely due to significant localized electron density on the pyridine ring. A DEPT-135 experiment was employed to confirm this resonance was not due to a $-CH_2$ (Figure S17); however, the carbon atoms in the plane of the pyridine ring did not produce an appreciable signal. We hypothesize these atoms are strongly affected both by the uranium as well as by the ligand radical, which enforce significant changes to τ_1. This is supported by the fact that atoms orthogonal to the pyridine ring were visible in the DEPT experiment. Significant charge localization on a single carbon would invariably result in observable distortion from sp^2 to sp^3, and *J*-coupling constants suggest the pyridine $C_{meta}-C_{para}-C_{meta}$ linkage is best described as allylic, $-C_{meta}H{=}C_{para}H-C_{meta}H-$, rather than aromatic, as the doublet of triplets observed for $C_{para}-H$ (J = 3.9, 9.9 Hz) is inconsistent with aromatic ortho coupling. Variable-temperature ^{1}H NMR spectroscopic data obtained in the range from −100 to 75 °C showed only minimal shifting of the resonances (Figure S13). As the temperature is decreased from 75 °C, those resonances arising from protons coplanar with the pyridine ring shift consistently upfield (∼0.3 ppm) while those resonances attributable to either the Cp* or the mesityl groups remain relatively constant.

Solid state characterization of **3** was performed through analysis of blue crystals by X-ray crystallography. Refinement of the data (λ = 1.54184 Å, 150 K) revealed a pseudo-octahedral uranium center with an η^5-Cp* ligand, a tridentate pyridine-(diimine) ligand, and *trans* terminal oxos (Figure 2). In contrast

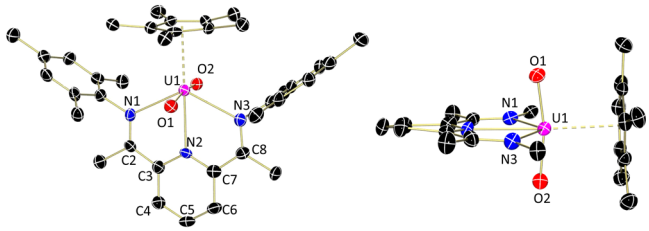

Figure 2. Molecular structure of **3** (150 K, λ = 1.54184 Å) displayed at 30% probability ellipsoids. Hydrogen atoms and aryl substituents (right) have been omitted for clarity.

to Cp*U(^{Mes}PDI^{Me})(THF),[18] where the uranium center is deviated from the plane of the ^{Mes}PDI^{Me} ligand by 1.059 Å, the uranium is coplanar with ^{Mes}PDI^{Me} in **3**. The centroid of the η^5-Cp* ring is calculated to be 2.583 Å from the uranium center, on the order of other uranium(VI) complexes, including Cp*$_2$U(=NAd)$_2$ (2.584, 2.615 Å)[28] and [Et_4N]$_2$[Cp*$UO_2(CN)_3$] (2.568 Å).[27] Steric pressure from the large Cp* ring causes a significantly distorted O=U=O bond angle (168.4(2)°) from the linearity typical of uranyl complexes, similar to that observed for [Et_4N]$_2$-[Cp*$UO_2(CN)_3$] (168.40°).[27] The U=O bonds in **3** (1.791(5) and 1.799(5) Å) are on the order of those of other hexavalent uranyl complexes that possess bent O=U=O angles including [$C(Ph_2PS)_2$]$UO_2(pyr)_2$ (1.783 Å, 171.81°),[29] [$C\{Ph_2PN(C_6H_2Me_3)_2\}_2$]$UO_2(Cl)(THF)$ (1.779 Å, 173.81°),[30] [2,6-(Me_2NCH_2)(NC_5H_3)]$UO_2(H_2C(o\text{-}PhO)_2)$ (1.798 Å, 172.52°),[31] and $(pyr)_2UO_2(N(SiMe_3)_2)_2$ (1.779 Å, 170.49°).[32] The U−N bonds of 2.504(6), 2.529(6), and 2.547(6) Å for the pyridine(diimine) ligands are much longer than those in **1**, supporting three dative bonding interactions.[18] However, ligand reduction is apparent by examining the intraligand distances for the pyridine ring. As is the case for the previously reported [^{Mes}PDI^{Me}]$^{1-}$ complex, Cp*U-($O_2C_2Ph_2H_2$)(^{Mes}PDI^{Me}),[33] significant elongation is observed in the C3−C4 and C6−C7 bonds (1.487(11) and 1.471(11) Å, respectively), indicating a ligand radical.

To further support the hypothesis of a [^{Mes}PDI^{Me}]$^{1-}$ ligand, crystallographic data for complex **3** were collected employing both molybdenum (λ = 0.71073 Å) and copper (λ = 1.54184 Å) X-ray sources. Full data sets were collected for two crystals, each from independently synthesized samples. Both analyses gave the same result (Table 1, Table S1), eliminating the possibility of additional hydrogen atoms on the ligand,

DOI: 10.1021/jacs.5b06217
J. Am. Chem. Soc. 2015, 137, 11115−11125

consistent with the solution NMR spectroscopic studies. The presence of a $^{Mes}PDI^{Me}$ ligand radical requires that, by charge balance considerations, compound **3** contains a uranium(VI) ion. This ligand radical is likely the source of the intense blue color of **3**, as closed shell U(VI) uranyl complexes generally have colors in the red to yellow-green range (vide infra).

Formation of the *trans*-dioxo unit from a uranium(IV) species is quite rare, as this typically requires a four-electron uranium-centered oxidation event. Kiplinger and co-workers showed the utility of a flexible PNP pincer ligand (PNP = bis[2-(diisopropylphosphino)-4-methylphenyl]amido) to form $(PNP)_2UO_2$ from a low-valent precursor ($(PNP)_2UI + KC_8$) and external oxidant (pyridine *N*-oxide).[34] Similarly, Mazzanti et al. were able to access a stable pentavalent−uranyl coordination polymer, $\{[UO_2(pyr)_5][KI_2(pyr)_2]\}_n$, from the addition of pyridine *N*-oxide and water to $UI_3(THF)_4$. In the case of **3**, access to stored electron density in the redox-active pyridine(diimine) allows for uranyl construction, circumventing a four-electron oxidation of uranium. Two electrons are transferred from uranium, while the other two electrons are derived from the reduced $[^{Mes}PDI^{Me}]^{3-}$ ligand.

Variations to both the $^{Mes}PDI^{Me}$ framework as well as the bound Lewis base were explored to determine how these modifications would influence the reaction to form **3** as well as the resulting electronic structure. To generate a more electron-rich system, a $^{Mes}PDI^{Me}$ ligand with an electron-donating *tert*-butyl group in the *p*-pyridine position was synthesized (ΔE_{red} = 124 mV, Figure S5). Raising the reduction potential of the ligand could prevent electron storage and facilitate isolation of the pentavalent uranyl analogue of $Cp^*U(NPh)_2(^{Mes}PDI^{Me})$.

Installation of a *tert*-butyl moiety at the 4 position of the pyridine ring to form 2,6-((Mes)N=CMe)$_2$-*p*-C(CH$_3$)$_3$-C$_5$H$_2$N (**^{t}Bu-^{Mes}PDI^{Me}**) was achieved following procedures similar to those by Burger and co-workers.[25] Metalation of **^{t}Bu-^{Mes}PDI^{Me}** with uranium was achieved following a similar protocol used in the generation of $Cp^*U(^{Mes}PDI^{Me})(THF)$ (**1**), eq 2,[18] forming

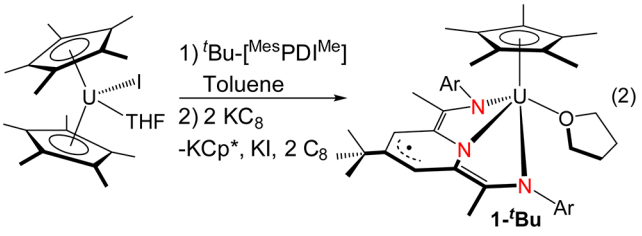

$Cp^*U(^tBu\text{-}^{Mes}PDI^{Me})(THF)$ (**1-^{t}Bu**) following workup. Similar to the ^{1}H NMR spectrum for **1**, **1-^{t}Bu** displays a sharp, paramagnetically shifted, asymmetric spectrum containing 20 resonances (Figure S6) with the two largest at −2.55 (15H) and −3.78 (9H) ppm assignable to Cp* and *tert*-butyl substituents, respectively. The remaining resonances are assignable to the C*H* and C*H*$_3$ groups of ^{t}Bu-^{Mes}PDI^{Me} and the methylene protons of a THF ligand.

In order to determine structural distortions in the ligand from reduction, single crystals of **1-^{t}Bu** obtained from a concentrated diethyl ether solution at −35 °C were analyzed. Refinement of the crystallographic data confirmed the formation of $Cp^*U(^tBu\text{-}^{Mes}PDI^{Me})(THF)$ (**1-^{t}Bu**) with an η^5-cyclopentadienyl ring (U1−Ct = 2.553 Å) and THF (U1−O1 = 2.540(3) Å) (Figure 3) related by a mirror plane. Short uranium−nitrogen distances (U1−N1 = 2.293(2) Å; U1−N2 = 2.204(3) Å) suggest a $[^{Mes}PDI^{Me}]^{3-}$ ligand in analogy to **1**.[18]

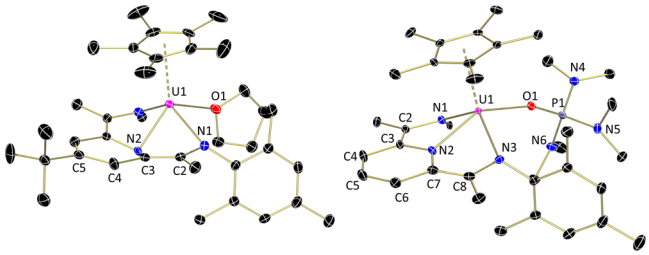

Figure 3. Molecular structures of **1-^{t}Bu** (left) and **1-HMPA** (right) displayed at 30% probability ellipsoids. Hydrogen atoms, selected aryl substituents, and a second molecule in the unit cell have been omitted for clarity.

Intraligand bond distances support ligand reduction, with an elongated N−C$_{imine}$ bond (N1−C2 = 1.418(4) Å) on the order of a single bond, while the adjacent C−C bond (1.372(4) Å) shows significant contraction to a double bond. The molecular structure of **1-^{t}Bu** also shows the uranium is 1.032 Å above the plane of the three nitrogen atoms, which is similar to the value found for **1** of 1.059 Å.

With a trianionic $[^{Mes}PDI^{Me}]^{3-}$ ligand, charge balance considerations point to **1-^{t}Bu** containing a uranium(IV) ion, analogous to **1**. This was corroborated by the electronic absorption spectrum for **1-^{t}Bu**, which was nearly identical to **1** with sharp f−f transitions of weak intensity (50−120 M^{-1} cm^{-1}) observable between 2100 and 1000 nm (Figure S8).

With **1-^{t}Bu** in hand, efforts were aimed at the synthesis of the corresponding uranyl species. Using the same procedure as for **1**, addition of NMMO (2 equiv) to **1-^{t}Bu** produced the analogous species, $Cp^*UO_2(^tBu\text{-}^{Mes}PDI^{Me})$ (**3-^{t}Bu**), as a dark blue solid. The ^{1}H NMR spectrum of **3-^{t}Bu** displays a similar C_s distribution with the largest two resonances assigned to the Cp* ligand (4.51 ppm) and *tert*-butyl moiety (1.01 ppm). Singlets arising from the pyridine aryl protons largely deviate from one another (6.21, 3.76 ppm), and their respective ^{13}C resonances are shifted to 114.45 and 28.33 ppm. On the basis of the unusual blue color and spectroscopic features, **3-^{t}Bu** is assigned as U(VI) with a ^{t}Bu-^{Mes}PDI^{Me} radical, rather than the targeted pentavalent analogue.

Analysis of blue crystals of **3-^{t}Bu** by X-ray crystallography was performed to establish the absolute configuration and ligand reduction. Refinement of the crystallographic data (λ = 1.54184 Å, 200 K) revealed an analogous Cp* uranyl complex (U1−Ct = 2.588 Å) containing a mirror plane (coplanar with pyridine) with similar deviation from linearity of the O═U═O moiety (167.4(4)°) and uranium−oxygen bond lengths (U1−O1 = 1.766(10) Å) (Figure S20) as observed for **3**. Both **3** and **3-^{t}Bu** represent monomeric uranyl complexes with some of the largest deviations from linearity reported.[27,29,35] While **3** also displays significant distortions within the pyridine ring, **3-^{t}Bu** contains a pyridine ring with a lesser degree of distortion. However, the crystal data suggest reduction of one imine arm (2.417(8) Å, U1−N1), consistent with a $^{Mes}PDI^{Me}$ radical. The other distances (2.548(9) Å, U1−N2; 2.603(9) Å, U1−N3) are analogous to those for **3**.

Alteration of the pyridine ring did not change the reaction or the electronic structure of the resulting uranyl species; however, replacement of the weakly bound tetrahydrofuran ligand in **1** with a strongly donating HMPA ligand did, generating $Cp^*U(^{Mes}PDI^{Me})(HMPA)$ (**1-HMPA**). Similar to **1** and **1-^{t}Bu**, **1-HMPA** produces an asymmetric paramagnetically shifted ^{1}H NMR spectrum containing 17 resonances, the

DOI: 10.1021/jacs.5b06217
J. Am. Chem. Soc. 2015, 137, 11115−11125

largest two assigned to the Cp* (−2.20 ppm) and HMPA (doublet, 0.02 ppm). Despite the paramagnetism, the HMPA ligand shows a broad resonance in the ^{31}P NMR spectrum at 164.9 ppm. Structural parameters of **1-HMPA** were obtained by analysis of single X-ray-quality crystals obtained from a concentrated THF/diethyl ether solution (10:1) at −35 °C. Refinement of the data revealed the anticipated pyridine-(diimine) uranium pentamethylcyclopentadienyl (U1−Ct = 2.539 Å) complex bound by a dative hexamethylphosphoric triamide ligand (U1−O1 = 2.339(2) Å) (Figure 3, Table 1). The uranium−oxygen distance, as expected, is significantly shorter in **1-HMPA** as compared to the parent complex (U−O_{THF} = 2.474(2) Å), signifying a stronger interaction. Three short uranium nitrogen distances (2.338(3), 2.234(3), and 2.333(3) Å) are again suggestive of a trianionic chelate, and intraligand distances support this. For **1-HMPA**, the uranium center is situated 1.015 Å above a plane defined by the three $[^{Mes}PDI^{Me}]^{3-}$ nitrogen atoms.

Interestingly, upon addition of 2 equiv of NMMO to **1-HMPA** to generate **3**, a gradual color change first to dark green (~2 min) was noted on the way to form dark blue **3** (eq 3).

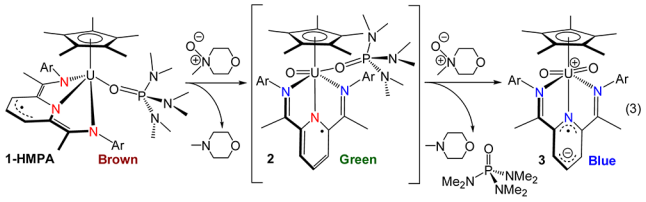

Due to the stronger bonding of HMPA over THF, we hypothesized the intermediate green compound may be due to the transfer of a single $[O]^{2-}$ to form the mono-oxo complex, Cp*UO(^{Mes}PDI^{Me})(HMPA) (**2**). It was possible to observe **2** spectroscopically in situ by generating it in neat HMPA with a substoichiometric amount of NMMO. The C_s-symmetric ^{1}H NMR spectrum with resonances ranging from −12.98 to 85.60 ppm is consistent with the mono-oxo formulation, with large resonances noted for the Cp* (−3.18 ppm) and HMPA (−12.98 ppm) ligands. The furthest downfield-shifted resonance (85.60 ppm) is consistent with the imine methyl substituents of a reduced $[^{Mes}PDI^{Me}]^{1-}$ ligand similar to that observed for $Cp^{P}U(X)_2(^{Mes}PDI^{Me})$ (Cp^{P} = 1-(7,7-dimethylbenzyl)cyclopentadienide; X = I, Cl, SPh, SePh, TePh) (Figure S11).

The electronic absorption spectrum of **2** shows a near-infrared region that is significantly different from **1**, **1-^{t}Bu**, and **1-HMPA** that maintains sharp, weak bands characteristic of a uranium(IV) 5f^2 center (Figure S10). The visible spectrum of **2** displays a notable absorbance at ca. 440 nm, which contrasts **1-HMPA**, as well as a local minimum at 512 nm that can be attributed to the green color. Uranium mono(oxo) complexes are precedented but limited to species whose precursors disallow the addition of trans substituents, such as Tp*$_2$U(2,2′-bpy)[36] (2,2′-bpy = bipyridyl; Tp* = hydrotris(3,5-dimethylpyrazolyl)borate) and Cp′$_2$U(2,2′-bpy)[37] (Cp′ = 1,2,4-tri-*tert*-butylcyclopentadienide), or do not have two oxidizable electrons such as Cp*$_2$U(NAr)(O)(L)[38] (Ar = Ph, 2,4,6-Me$_3$C$_6$H$_2$, 2,6-diisopropylphenyl, 2,4,6-^{t}Bu-C$_6$H$_2$; L = Li(TMEDA)Cl, NC$_5$H$_5$, THF), (NN′$_3$)UO[39] (NN′$_3$ = N(CH$_2$CH$_2$NSiMe$_2$^{t}Bu)$_3$), and U[N(SiMe$_3$)$_2$]$_3$(O).[40]

The uranyl complexes were investigated by vibrational spectroscopy to determine the relative energetics of the diagnostic O═U═O vibration. Infrared spectroscopy revealed both strong (**3**, 876 cm^{-1}; **3-^{t}Bu**, 878 cm^{-1}) and weak vibrations (787 cm^{-1}, both) assigned to the $\upsilon_{O=U=O}$ asymmetric and symmetric stretches, respectively (Figure 4,

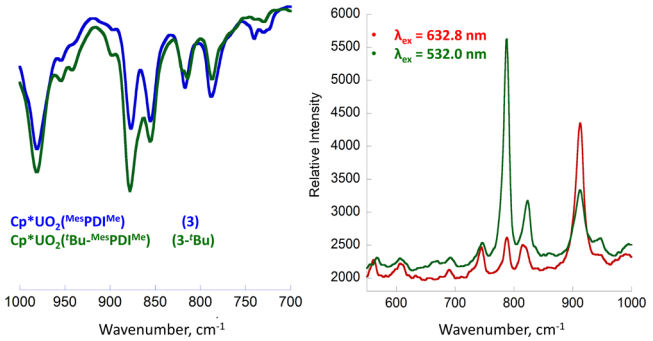

Figure 4. (Left) Infrared spectra of **3** (blue) and **3-^{t}Bu** (green). (Right) Resonance Raman spectra of **3** at excitation wavelengths of 632.8 (red) and 532 nm (green).

left). Further confirmation of the symmetric stretch in complex **3** was achieved via resonance Raman spectroscopy, which showed an absorption at 788 cm^{-1} from excitation at λ = 632.8 nm. This assignment was confirmed by employing an excitation source (532.0 nm) nearer to the observed O → U ligand-to-metal charge transfer band (vide infra), which resulted in significant amplification of this signal (Figure 4, right). The Raman shift of the symmetric uranyl stretch for complex **3-^{t}Bu** was observed at 789 cm^{-1} (λ_{ex} = 1064 cm^{-1}; Figure S22). Similar symmetric and asymmetric stretching frequencies for uranyl complexes are observed in Schiff base ligand systems, including UO$_2$(sal-*p*-phdn)(H$_2$O) (υ_{asym} = 915; υ_{sym} = 830 cm^{-1}) (sal-*p*-phdn = *N*,*N*′-*p*-phenylene-bis(salicylideneiminato))[41] and UO$_2$(NCS)$_2$(Me-N-Sal)$_3$(H$_2$O)$_2$ (υ_{asym} = 912; υ_{sym} = 822 cm^{-1}) (Me-N-Sal = *p*-CH$_3$-salicylideneaniline).[42] Crystallographically characterized Schiff base uranyl adducts show a decrease in frequency correlated to a reduction in the O−U−O angle from 180°, including UO$_2$(NAC) (υ_{asym} = 897 cm^{-1}; O═U═O = 172.3°) (H$_2$NAC = [(MeO)$_2$CH−HOC$_6$H$_2$Cl−CH═(CH$_2$)$_2$]$_2$NH)[43] and UO$_2$(L)(NC$_5$H$_4$-*p*-C$_4$H$_9$) (υ_{asym} = 899 cm^{-1}; O═U═O = 171.8°) (L = 3,3′-[1,2-phenylene-bis(nitrilomethylidyne)]bis[2′-methoxy-[1,1′-biphenyl]-2-olato]),[44] which compare favorably with the degree of bending observed in **3** and **3-^{t}Bu**.

Due to the bright blue colors of **3** and **3-^{t}Bu**, investigation by electronic absorption spectroscopy was also performed. Both complexes exhibit three strong absorbances in the UV−vis region (Figure 5). The intense LMCTs from the O═U═O moiety at 344 nm (ε = 10 694 M^{-1} cm^{-1}) and 346 nm (ε = 7143 M^{-1} cm^{-1}) for **3** and **3-^{t}Bu**, respectively, are shifted to significantly higher energy from a standard [UO_2^{2+}] ion (ca. 420 nm).[45] This blue shift is consistent with the decreased O═U═O stretching frequency observed as a result of bending (vide supra). The other two absorbances in each complex are proposed to arise from pyridine(diimine) anion transitions analogous to that previously observed in Cp*U(O$_2$C$_2$Ph$_2$H$_2$)(^{Mes}PDI^{Me})[33] and like transitions seen for the ferrocenyl−perchlorotriphenylmethyl vinylene-bridged platform studied by Veciana and co-workers.[46] The dominant color producing band in **3-^{t}Bu** (620 nm, 7400 M^{-1} cm^{-1}) is slightly red shifted from that of **3** (611 nm, 11 439 M^{-1} cm^{-1}). Neither complex

DOI: 10.1021/jacs.5b06217
J. Am. Chem. Soc. 2015, 137, 11115−11125

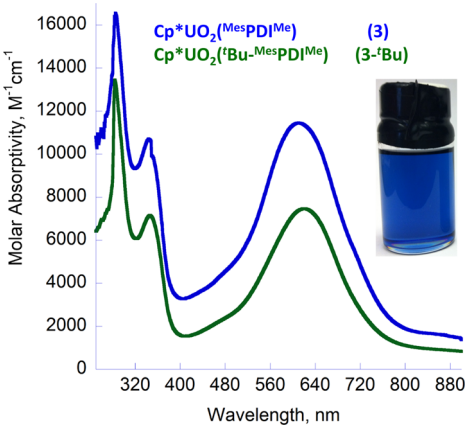

Figure 5. Electronic absorption spectra of **3** (blue) and **3-^{t}Bu** (green) recorded from 260 to 900 nm in toluene at 25 °C. (Inset) Toluene solution of **3** (approximately 10^{-5} M).

displayed transitions in the near-infrared region, suggesting U(VI) $5f^0$ complexes (Figure S18).

The ligand radical character in both **3** and **3-^{t}Bu** to generate a U(VI)/PDI^{1-} system has been corroborated by asymmetry in the ^{1}H NMR spectrum, bond distortions in the solid state structure, and intense visible features in the electronic absorption spectra. To further rule out the formulation of these species as U(V) with neutral PDI^0 chelates, EPR spectroscopy was employed. Although both systems contain an unpaired electron, differentiation between a uranium-centered and a ligand-centered radical should be possible by measurement at room temperature. Uranium $5f^1$ systems have been thoroughly studied[47] and are generally known to be EPR silent above liquid nitrogen temperatures.[48] For example, Cummins and co-workers found the hexakisamidouranium(V) complex $[Li(THF)_x][U(dbabh)_6]$ (Hdbabh = 2,3:5,6-dibenzo-7-azabicyclo[2.2.1]hepta-2,5-diene) to be EPR silent at room temperature but active at both 20 and 100 K, producing a broad isotropic signal centered at |g| = 1.12 in frozen acetonitrile/toluene.[49] To the contrary, pyridine(diimine) ligand radicals have been observed at room temperature on alkali,[50] main group,[51] and transition metals.[52,53] Solutions of both **3** (toluene, 6 mM) and **3-^{t}Bu** (*n*-pentane, 6 mM) at 293 K produce an isotropic signal diagnostic of an $S = 1/2$ system centered at |g| = 1.974 and 1.936, respectively (Figure 6). The experimental *g* value is significantly shifted from that reported

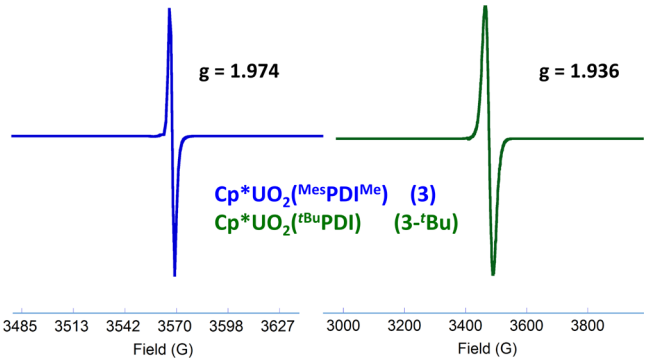

Figure 6. EPR spectra of **3** (left, toluene, 6 mM) and **3-^{t}Bu** (right, *n*-pentane, 6 mM) recorded at 25 °C. Frequency: 9.417 GHz. Power: 10.0 mW. Modulation: 0.5 mT/100 kHz.

by Chirik and co-workers for singly reduced pyridine(diimine) free ligand (2.003),[53] suggesting the ligand radical is associated with uranium but is not localized there. While both hydrogen and nitrogen superhyperfine coupling are observed in (^{iPr}PDI)-$Al(CH_3)_2$[51] (^{iPr}PDI = 2,6-[2,6-(^{i}Pr)$_2$C$_6$H$_3$N=C-(CH$_3$)]$_2$(C$_5$H$_3$N)) as well as the free ligand,[53] the spectra for complexes **3** and **3-^{t}Bu** lack such splitting. Similarly, Chirik and co-workers observed neither nitrogen nor hydrogen superhyperfine coupling in (^{iPr}PDI)Co(N$_2$).[53] The observed EPR signal suggests that **3** and **3-^{t}Bu** can most appropriately be described as hexavalent uranyl species with ligand radicals.

The electronic structure of **3** (and related compounds) was surprising, given that the corresponding imido analogue, Cp*U(NPh)$_2$(^{Mes}PDI^{Me}),[18] is pentavalent with a neutral ligand. In the formation of **3**, two electrons are oxidized from both U and [^{Mes}PDI^{Me}]$^{3-}$, whereas for Cp*U(NPh)$_2$(^{Mes}PDI^{Me}), three-electron oxidation occurs at [^{Mes}PDI^{Me}]$^{3-}$, forming [^{Mes}PDI^{Me}]^0, but only a one-electron oxidation occurs at uranium. With the major difference between these being substitution of oxo ligands for −NPh units, the dichotomy in the electronic structures points toward the phenyl(imido) substituents being more electron withdrawing than the oxo, thus siphoning electron density from the ^{Mes}PDI^{Me} ligand framework. This is consistent with our earlier finding in which the tris(imido) analogue, (^{Mes}PDI^{Me})U(NMes)$_3$, was shown to have less covalent-bond character in the U−element multiple bonds as compared to the tri(oxo) analogue, (^{Mes}PDI^{Me})UO$_3$, which can also be attributed to the superior electron-withdrawing ability of the mesityl(imido) substituents.

In terms of their electronic structures, complexes **3** and **3-^{t}Bu** are similar to [UO$_2$(gha)(dmso)]$^-$.[16] Due to its instability, [UO$_2$(gha)(dmso)]$^-$ was generated and detected by spectroelectrochemical reduction of [UO$_2$(gha)(dmso)] (reversible −1.194 V (vs Fc/Fc$^+$)). Identification was possible due to the lack of absorption in the range of 900−1900 nm that would be expected for a uranium(V) center. The cyclic voltammogram of **3** shows an irreversible wave at −0.287 V (vs Fc/Fc$^+$, Figure S23), tentatively assigned to a U(VI)[^{Mes}PDI^{Me}]$^{1-}$/U(VI)-[^{Mes}PDI^{Me}]^0 oxidation, establishing that **3** is significantly more difficult to oxidize than [UO$_2$(gha) (dmso)]$^-$. Like [UO$_2$(gha)-(dmso)]$^-$, no absorptions characteristic for f−f transitions for **3** or **3-^{t}Bu** were noted in the NIR region, supporting formation of a uranium(VI) ion. For [UO$_2$(gha)(dmso)]$^-$ charge balance considerations point to ligand reduction in the form of a glyoxal ligand radical, which is supported computationally. The calculated spin density on the ligand of 0.735 is expected for a reduced glyoxal, while the corresponding value for uranium was calculated to be ∼0 (−0.0141). Further evidence for the uranium(VI) oxidation state in [UO$_2$(gha)(dmso)]$^-$ was obtained through comparison of the computed symmetric and asymmetric uranyl vibrations with the parent UO$_2$(gha)-(dmso). The data obtained showed overall minimal decreases (Δ = 27 and 30 cm^{-1}, respectively), which are not extreme enough to indicate a change in oxidation state at uranium.[16] Thus, **3** and **3-^{t}Bu** are significant as they are the first *isolated* examples of uranyl complexes supported by ligand radicals for full characterization.

Reactivity of Uranyl Complexes. Due to the unusual electronic structure of **3** and **3-^{t}Bu** as well as the bent and subsequently activated [UO$_2$]$^{2+}$ unit, studies aimed at activating the robust [UO$_2$]$^{2+}$ core with silylhalides were commenced. Treating **3** with 2 equiv of Me$_3$SiI resulted in a color change from bright blue to purple and progressed to dark red over 24 h

DOI: 10.1021/jacs.5b06217
J. Am. Chem. Soc. 2015, 137, 11115−11125

Scheme 1. Reductive Silylation of Cp*UO_2($^{Mes}PDI^{Me}$) (3)

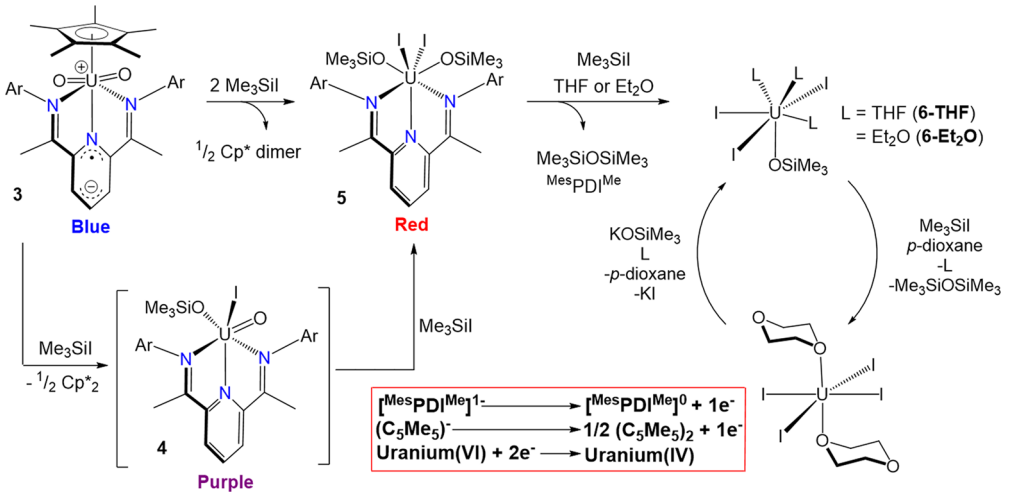

(Scheme 1). Following workup and isolation, analysis by ^{1}H NMR spectroscopy revealed a paramagnetic uranium compound with seven broadened resonances ranging from −9.26 to 20.31 ppm in C_{2v} symmetry (Figure S25). Interestingly, investigation of the organic byproducts revealed formation of 0.5 equiv of Cp* dimer. Consequently, the largest resonance of the organometallic species (18H, 11.21 ppm) was assigned as equivalent trimethylsilyl functionalities. The presence of trimethylsiloxy substituents was further confirmed via infrared spectroscopy by their characteristic symmetric (1246 cm^{-1}) and asymmetric (840 cm^{-1}) bending modes.[54] The remaining six resonances in the ^{1}H NMR spectrum were assigned to the symmetric $^{Mes}PDI^{Me}$ ligand, suggesting the product to be $(Me_3SiO)_2UI_2(^{Mes}PDI^{Me})$ (**5**).

Absolute structural confirmation of **5** was achieved by X-ray diffraction of red crystals that precipitated from a dilute benzene solution at room temperature. Refinement of the data revealed **5** to be a seven-coordinate, pentagonal bipyramidal uranium species with *trans*-trimethylsiloxide ligands, *cis*-iodides, and a tridentate pyridine(diimine) (Figure 7, structural parameters in Table 1). The U−O distances of 2.091(10) and 2.098(10) Å are on the order of those for a uranium(IV) species with siloxide ligands, similar to $[\eta^5$-1,2,4-$(Me_3C)_3C_5H_2]_2UI(OSiMe_3)$ (2.104(4) Å),[37] $[U(OSiMe_3)(NR_2)_2]_2(RNSiMe_2CH_2)_2$ (R = $SiMe_3$) (U−O = 2.102(2) Å),[55] $U(OSiMe_3)_2I_2(bipy)_2$ (U1−O1 = 2.084(4) Å),[56] and $[U(OSiMe_3)_2I(THF)_4][I_3]$ (U1−O1 = 2.065(6), U1−O2 = 2.080(6) Å),[56] which were all formed by oxo silylation. The U−N distances in **5** of 2.737(9) and 2.605(13) Å are longer than those reported in the neutral pyridine(diimine)uranium(IV) complex $(^{Mes}PDI^{Me})UI_2(NMes)(THF)$,[17] supporting a dative coordination of the chelate. Thus, the ligand radical is no longer present, as confirmed by structural parameters, nor were additional protons noted on the pyridine ring. The U−I distance of 3.0992(9) Å is consistent with those observed in $UI_4(1,4\text{-dioxane})_2$.[22] In forming **5**, reduction from U(VI) to U(IV) occurs. This finding is significant as the majority of reported reductive silylation reactions only result in a single reduction of the metal center. One reducing equivalent is provided by the $[^{Mes}PDI^{Me}]^{1-}$, and the second equivalent is gained through the homolytic bond cleavage of the cyclopentadienyl−uranium bond. The loss of Cp^*_2 has been observed by Evans and co-workers and utilized as a convenient

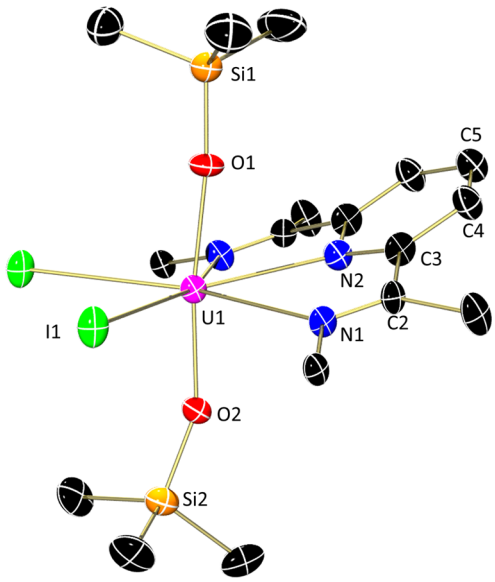

Figure 7. Molecular structure of **5** displayed at 30% probability ellipsoids. Hydrogen atoms, aryl substituents, cocrystallized benzene molecules, and second unit in the asymmetric cell have been omitted for clarity.

source of an electron for bond activation studies of a variety of substrates with both lanthanides[57,58] and actinides.[59,60]

The formation of **5** is significant, as a well-defined system for the *stoichiometric* functionalization of a uranyl unit is exceedingly rare. Typically, an excess of silylating reagent is required, as in the cases of $UO_2(^{tBu}acnac)_2$[56] and $UO_2(^{Ar}acnac)_2$.[7] However, stoichiometric reductive silylation of these and the bis(acnac) systems was accomplished using silanes and the strong Lewis acid $B(C_6F_5)_3$, which serves to preactivate the Si−H bonds, forming the uranium(V) species $(Ph_3SiO)U(OB\{C_6F_5\}_3)(^{Ar}acnac)_2$[10] or $[(Et_3SiO)_2U(^{Ar}acnac)_2][HB(C_6F_5)_3]$.[11,12] Similar functionalization was possible by taking advantage of the highly reactive Ph_3Si−OTf, which generated $(Ph_3SiO)_2U(acac)_2(OTf)$.[15]

With stoichiometric silylation of **3** achieved, full removal of the oxo groups was attempted. Treating **3** with 3 equiv of Me_3SiI allowed for isolation of a brown/green powder after recrystallization from THF/*n*-pentane (Scheme 1). Inspection

DOI: 10.1021/jacs.5b06217
J. Am. Chem. Soc. 2015, 137, 11115−11125

of the organic byproducts by ^{1}H NMR spectroscopy revealed the formation of 1 equiv of $Me_3SiOSiMe_3$ as well as the release of $[^{Mes}PDI^{Me}]^0$. Again, no additional protons were found on the pyridine ring of the released ligand. The uranium product gave a spectrum containing one sharp (50.74 ppm) and one broad resonance (−6.18 ppm) in a ratio of 9:24, suggesting the product to be $(Me_3SiO)UI_3(THF)_3$ (**6-THF**) (Figure S27). Complex **6** was independently synthesized by the addition of $KOSiMe_3$ to a diethyl ether solution of $UI_4(p\text{-dioxane})_2$, producing the etherate adduct, $(Me_3SiO)UI_3(Et_2O)_3$ (**6-Et$_2$O**). Complex **6-Et$_2$O** gives a similar ^{1}H NMR spectrum with a single sharp resonance (51.68 ppm) assigned to the $-Si(CH_3)_3$ along with two broad resonances assigned to coordinated diethyl ether (−14.33, 12H; −9.08 ppm, 18H) (Figure S29). Complexes **6-THF** and **6-Et$_2$O** exhibit chemical shifts similar to the analogous aryloxide compound, $(C_6H_5O)UI_3(THF)_3$.[26]

Cleavage of the second oxo functionality was achieved by the addition of an equivalent of Me_3SiI to **6** in *p*-dioxane producing $UI_4(1,4\text{-dioxane})_2$ (Scheme 1). Monitoring the reaction by ^{1}H NMR spectroscopy (C_6D_6 with 0.200 mL of Et_2O) revealed the disappearance of the paramagnetically shifted $-Si(CH_3)_3$ resonance concomitant with the formation of $Me_3SiOSiMe_3$ and $UI_4(Et_2O)_2$. While the oxo cleavage in **3** was accomplished using Me_3SiI, Hayton and co-workers successfully cleaved their oxo-derived ligand via protonolysis of $(R_3SiO)U(OB\{C_6F_5\}_3)(dbm)_2(THF)$ (R = Ph, Et; dbm = dibenzoylmethanate) with an additional equivalent of Hdbm to yield triethylsilanol and the tris(ligand) derivative $(\{C_6F_5\}_3BO)U(dbm)_3$.[11]

The uranium(IV) oxidation state in complexes **5** (Figure S32) and **6-Et$_2$O** (Figure S29) was further confirmed by electronic absorption spectroscopy. Both complexes display weakly intense (ε = 20−60 M^{-1} cm^{-1}) sharp f−f transitions throughout the near-infrared region and for **6-Et$_2$O** well into the visible region, indicative of uranium(IV) $5f^2$ complexes. Complex **5** displays a strong color producing band (λ_{max} = 485 nm; ε = 11 471 M^{-1} cm^{-1}) assigned to a pyridine(diimine)-based transition (vide infra) and a slightly weaker, higher energy band (λ_{max} = 370 nm; ε = 7171 M^{-1} cm^{-1}), while the only strong absorbance in **6-Et$_2$O** is nearly an order of magnitude weaker (λ_{max} = 345 nm; ε = 1596 M^{-1} cm^{-1}).

During the formation of **5**, a color change from blue to purple and finally to red was noted. The potential of this purple color to represent an intermediate (**4**) in the progression of **3** to **5** was investigated by monitoring the reaction of **3** with a single equivalent of Me_3SiI. ^{1}H NMR spectroscopy indicated the loss of Cp^*_2 occurs initially with the appearance of paramagnetically shifted resonances assignable to neither **3** nor **5** but an intermediate, **4**. Complex **3** is stable in solution at room temperature for multiple days, suggesting the loss of Cp^*_2 is induced by the addition of Me_3SiI; therefore, **4** is not $UO_2(^{Mes}PDI^{Me})$. Unfortunately, the addition of a full equivalent of Me_3SiI at room temperature resulted in formation 0.5 equiv of **5** and 0.5 equiv of unreacted **3**, suggesting the second silylation occurs rapidly. Isolable quantities of **4** were synthesized by keeping the toluene reaction mixture cold (−35 °C) and layering it with *n*-pentane, resulting in the precipitation of **4** as a dark purple solid as it was formed. By this method, a ^{1}H NMR spectrum was attainable (Figure S24). The spectrum suggests an asymmetric complex in solution with paramagnetically shifted resonances ranging from −42.41 to 60.05 ppm accounting for a coordinated $^{Mes}PDI^{Me}$ ligand. Infrared spectroscopy confirmed the presence of an $-SiMe_3$ moiety by its symmetric and asymmetric bending modes (Figure S30). Unfortunately, the broadness of these absorbances precluded the assignment of a potential terminal U(IV)═O stretch. Due to the instability of **4**, further attempts at purification resulted in decomposition to intractable byproducts. On the basis of these results, intermediate **4** is hypothesized to be formed by homolytic cleavage of the uranium−Cp* with concomitant Me_3Si-I addition across one U═O bond and is assigned as $(Me_3SiO)UO(I)(^{Mes}PDI^{Me})$ (**4**).

Further evidence for **4** was achieved by monitoring the reaction to form **5** from **3** by electronic absorption spectroscopy in the UV−vis region (Figure 8). Upon addition of

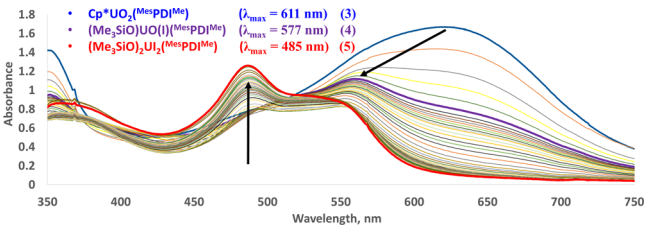

Figure 8. Electronic absorption spectrum (25 °C, toluene) monitoring the reaction between Me_3SiI and **3**. Arrows indicate reaction progress to first form **4** (purple) from **3** (blue) and finally formation of **5** (red).

iodotrimethysilane, the absorbance identified as **3** (blue line; λ_{max} = 611 nm; vida supra) is rapidly quenched and a new blue-shifted absorbance emerges (purple line; λ_{max} = 577 nm) assigned to **4**. As the reaction proceeds, the 577 nm absorbance decreases with the emergence of a new absorbance at 485 nm (red line) belonging to **5** (Figure S32). The lack of an isosbestic point in the formation of **5** from **3** indicates the formation of an intermediate species.

Complex **4**, $(Me_3SiO)UO(I)(^{Mes}PDI^{Me})$, is a similar intermediate to that in the synthesis of $[(Et_3SiO)_2U(^{Ar}acnac)_2][HB(C_6F_5)_3]$ from $UO_2(^{Ar}acnac)_2$, where the authors propose the uranium(V) mono-oxo $(Et_3SiO)UO(^{Ar}acnac)_2$ is formed, followed by the second silylation and hydride abstraction by the Lewis acid to form product.[12]

Reductive silylation of **3-^{t}Bu** was achieved using the analogous synthetic protocol. Addition of 2 equiv of Me_3SiI to **3-^{t}Bu** resulted in a dark green solution within 30 min, followed by conversion to brown $(Me_3SiO)_2UI_2(^tBu\text{-}^{Mes}PDI^{Me})$ (**5-^{t}Bu**) after 1 h. ^{1}H NMR spectroscopy of **5-^{t}Bu** revealed a paramagentically shifted spectrum similar to **5** with the $-Si(CH_3)_3$ and $-C(CH_3)_3$ resonances located at 11.42 and 4.47 ppm, respectively. In analogy to **3**, addition of a third equivalent of Me_3SiI to **3-^{t}Bu** produced **6-THF** after a similar workup procedure. The rapid conversion to **5-^{t}Bu**, in comparison to **5**, as well as a different intermediate color (green vs purple) suggests that the tridentate ligand remains coordinated throughout the course of the reaction and that the electronics of the pyridine(diimine) ligand indeed play a role in the reactivity. Monitoring the reaction between **3-^{t}Bu** and Me_3SiI in the UV−vis region of the electronic absorption spectrum confirmed the absence of a band at ca. 577 nm akin to purple intermediate **4**. The green color qualitatively observed through the intermediate stage of the reaction is supported by a local minimum maintained in the region of ca. 510−525 nm. Despite the inability to observe a band attributable to intermediate **4-^{t}Bu**, the lack of an isosbestic point suggests the reaction does not proceed directly from **3-^{t}Bu** to **5-^{t}Bu** (Figure S33). While sharp, weakly intense transitions in the near-infrared region of **5-^{t}Bu** suggest a uranium(IV) complex

DOI: 10.1021/jacs.5b06217
J. Am. Chem. Soc. 2015, 137, 11115−11125

(Figure S32), confirmation of the expulsion of the ligand radical was by EPR spectroscopy (RT, toluene, 7 mM) (Figure S31) under a variety of settings, which did not produce a signal.

The observed silylation chemistry proceeds via efficient reduction of U(VI) to U(IV), with the reducing equivalents derived from both the pyridine(diimine) and the Cp* ligands. This is an exciting result in terms of extending uranyl fuctionalization, as reducing equivalents could be introduced from a variety of sources. Our studies also show that the initial functionalization of the first uranium−oxo is the most challenging, and once the strong *trans*-uranium dioxo unit (and corresponding inverse trans influence) is interrupted, functionalization of the second oxo proceeds readily, as does subsequent silylation of the resulting uranium−siloxy substituents to generate the uranium(IV) iodide derivatives.

CONCLUSION

In conclusion, a pair of hexavalent uranyl complexes have been synthesized via transfer of two $[O]^{2-}$ units from *N*-methylmorpholine *N*-oxide to highly reduced uranium complexes. Formation of a uranyl species via this route is rare, as the four-electron process is generally unreachable for uranium. Here, two reducing equivalents are derived each from the redox-active pyridine(diimine) ligand and the uranium(IV) metal center, contrary to what was previously observed in the formation of $Cp^*U(NPh)_2(^{Mes}PDI^{Me})$. While in-situ-generated uranyl U(VI)/$L^{\bullet-}$ has been observed previously, complexes **3** and **3-^{t}Bu** represent the first fully characterized uranium(VI) complexes bearing a ligand radical. Due to their stability, characterization by electronic absorption, vibrational, EPR, and multinuclear NMR spectroscopies as well as X-ray crystallography was possible.

Stoichiometric, stepwise reductive silylation of these uranyl complexes was accomplished using Me_3SiI to produce uranium(IV) siloxide complexes. As in the formation of the uranyl species, the redox-active pyridine(diimine) plays a significant role in the reductive silylation by providing a reducing electron while the second is derived from homolytic cleavage of the pentamethylcyclopentadienyl ligand. Thus, $Cp^*UO_2(^{Mes}PDI^{Me})$ can be thought of as a masked form of a tetravalent uranyl, which is highly active toward silylation. Further addition of Me_3SiI affords $UI_4(1,4\text{-dioxane})_2$ by full removal of the oxo groups, showing complete conversion from U(VI) to U(IV). Ongoing studies are focused on the scope of reagents available for the reductive silylation of the robust UO_2^{2+} core.

ASSOCIATED CONTENT

Supporting Information

The Supporting Information is available free of charge on the ACS Publications website at DOI: 10.1021/jacs.5b06217.

Crystallographic details (CIF)

Crystallographic details (CIF)

Crystallographic details (CIF)

Crystallographic details (CIF)

Crystallographic details (CIF)

Crystallographic details (CIF)

Additional experimental procedures, spectroscopic data, and crystallographic details (PDF)

AUTHOR INFORMATION

Corresponding Author

*sbart@purdue.edu

Author Contributions

The manuscript was written through contributions of all authors.

Notes

The authors declare no competing financial interest.

ACKNOWLEDGMENTS

The authors acknowledge support from the Division of Chemical Sciences, Geosciences, and Biosciences, Office of Basic Energy Sciences, Heavy Elements Chemistry Program of the U.S. Department of Energy through Grant DE-AC0212ER16328 (SCB). M.Z. thanks NSF Grant DMR 1337296 for X-ray diffractometer funding (used to collect the molecular structure for 1-HMPA).

REFERENCES

(1) Fortier, S.; Hayton, T. W. *Coord. Chem. Rev.* **2010**, *254*, 197−214.

(2) Reed, D. T.; Pepper, S. E.; Richmann, M. K.; Smith, G.; Deo, R.; Rittmann, B. E. *J. Alloys Compd.* **2007**, *444*−*445*, 376−382.

(3) Gil, D.; Malmbeck, R.; Spino, J.; Fanghaenel, T.; Dinnebier, R. *Radiochim. Acta* **2010**, *98*, 77−89.

(4) Depoorter, G. L.; Rofer-Depoorter, C. K. U.S. Patent US4080273A, 1978.

(5) Arnold, P. L.; Patel, D.; Wilson, C.; Love, J. B. *Nature* **2008**, *451*, 315−317.

(6) Berthet, J.-C.; Siffredi, G.; Thuery, P.; Ephritikhine, M. *Eur. J. Inorg. Chem.* **2007**, *2007*, 4017−4020.

(7) Brown, J. L.; Wu, G.; Hayton, T. W. *J. Am. Chem. Soc.* **2010**, *132*, 7248−7249.

(8) Arnold, P. L.; Hollis, E.; White, F. J.; Magnani, N.; Caciuffo, R.; Love, J. B. *Angew. Chem., Int. Ed.* **2011**, *50*, 887−890.

(9) Arnold, P. L.; Pecharman, A.-F.; Love, J. B. *Angew. Chem., Int. Ed.* **2011**, *50*, 9456−9458.

(10) Schnaars, D. D.; Wu, G.; Hayton, T. W. *Inorg. Chem.* **2011**, *50*, 4695−4697.

(11) Pedrick, E. A.; Wu, G.; Kaltsoyannis, N.; Hayton, T. W. *Chem. Sci.* **2014**, *5*, 3204−3213.

(12) Schnaars, D. D.; Wu, G.; Hayton, T. W. *Inorg. Chem.* **2011**, *50*, 9642−9649.

(13) Kannan, S.; Vaughn, A. E.; Weis, E. M.; Barnes, C. L.; Duval, P. B. *J. Am. Chem. Soc.* **2006**, *128*, 14024−14025.

(14) Graves, C. R.; Kiplinger, J. L. *Chem. Commun.* **2009**, 3831−3853.

(15) Pedrick, E. A.; Wu, G.; Hayton, T. W. *Inorg. Chem.* **2014**, *53*, 12237−12239.

(16) Takao, K.; Tsushima, S.; Ogura, T.; Tsubomura, T.; Ikeda, Y. *Inorg. Chem.* **2014**, *53*, 5772−5780.

(17) Anderson, N. H.; Odoh, S. O.; Yao, Y.; Williams, U. J.; Schaefer, B. A.; Kiernicki, J. J.; Lewis, A. J.; Goshert, M. D.; Fanwick, P. E.; Schelter, E. J.; Walensky, J. R.; Gagliardi, L.; Bart, S. C. *Nat. Chem.* **2014**, *6*, 919−926.

(18) Cladis, D. P.; Kiernicki, J. J.; Fanwick, P. E.; Bart, S. C. *Chem. Commun.* **2013**, *49*, 4169−4171.

(19) Pangborn, A. B.; Giardello, M. A.; Grubbs, R. H.; Rosen, R. K.; Timmers, F. J. *Organometallics* **1996**, *15*, 1518−1520.

(20) Mohammad, A.; Cladis, D. P.; Forrest, W. P.; Fanwick, P. E.; Bart, S. C. *Chem. Commun.* **2012**, *48*, 1671−1673.

(21) Chakraborty, S.; Chattopadhyay, J.; Guo, W.; Billups, W. E. *Angew. Chem., Int. Ed.* **2007**, *46*, 4486−4488.

(22) Monreal, M. J.; Thomson, R. K.; Cantat, T.; Travia, N. E.; Scott, B. L.; Kiplinger, J. L. *Organometallics* **2011**, *30*, 2031−2038.

(23) Sheldrick, G. M. *Acta Crystallogr., Sect. A: Found. Crystallogr.* **2008**, *64*, 112−122.

DOI: 10.1021/jacs.5b06217
J. Am. Chem. Soc. 2015, 137, 11115−11125

(24) Jutzi, P.; Kohl, F. *J. Organomet. Chem.* **1979**, *164*, 141−152.
(25) Nückel, S.; Burger, P. *Organometallics* **2001**, *20*, 4345−4359.
(26) Schnaars, D. D.; Wu, G.; Hayton, T. W. *Dalton Trans.* **2009**, 3681−3687.
(27) Maynadie, J.; Berthet, J.-C.; Thuery, P.; Ephritikhine, M. *Chem. Commun.* **2007**, 486−488.
(28) Warner, B. P.; Scott, B. L.; Burns, C. J. *Angew. Chem., Int. Ed.* **1998**, *37*, 959−960.
(29) Tourneux, J.-C.; Berthet, J.-C.; Cantat, T.; Thuéry, P.; Mézailles, N.; Ephritikhine, M. *J. Am. Chem. Soc.* **2011**, *133*, 6162−6165.
(30) Cooper, O. J.; Mills, D. P.; McMaster, J.; Tuna, F.; Mcinnes, E. J. L.; Lewis, W.; Blake, A. J.; Liddle, S. T. *Chem. - Eur. J.* **2013**, *19*, 7071−7083.
(31) Masci, B.; Thuery, P. *Acta Crystallogr., Sect. C: Cryst. Struct. Commun.* **2004**, *60*, m584−m586.
(32) Jones, G. M.; Arnold, P. L.; Love, J. B. *Chem. - Eur. J.* **2013**, *19*, 10287−10294.
(33) Kiernicki, J. J.; Newell, B. S.; Matson, E. M.; Anderson, N. H.; Fanwick, P. E.; Shores, M. P.; Bart, S. C. *Inorg. Chem.* **2014**, *53*, 3730−3741.
(34) Cantat, T.; Graves, C. R.; Scott, B. L.; Kiplinger, J. L. *Angew. Chem., Int. Ed.* **2009**, *48*, 3681−3684.
(35) Berthet, J.-C.; Thuery, P.; Dognon, J.-P.; Guillaneux, D.; Ephritikhine, M. *Inorg. Chem.* **2008**, *47*, 6850−6862.
(36) Kraft, S. J.; Fanwick, P. E.; Bart, S. C. *Inorg. Chem.* **2010**, *49*, 1103−1110.
(37) Zi, G.; Jia, L.; Werkema, E. L.; Walter, M. D.; Gottfriedsen, J. P.; Andersen, R. A. *Organometallics* **2005**, *24*, 4251−4264.
(38) Arney, D. S. J.; Burns, C. J. *J. Am. Chem. Soc.* **1995**, *117*, 9448−9460.
(39) Roussel, P.; Boaretto, R.; Kingsley, A. J.; Alcock, N. W.; Scott, P. *J. Chem. Soc., Dalton Trans.* **2002**, 1423−1428.
(40) Andersen, R. A. *Inorg. Chem.* **1979**, *18*, 1507−1509.
(41) Nour, E. M.; Alnaimi, I. S.; Alem, N. A. *J. Phys. Chem. Solids* **1992**, *53*, 197−201.
(42) Azeez, W. I.; Abdulla, A. I. *Inorg. Chim. Acta* **1985**, *110*, 15−18.
(43) Sitran, S.; Fregona, D.; Casellato, U.; Vigato, P. A.; Graziani, R.; Faraglia, G. *Inorg. Chim. Acta* **1987**, *132*, 279−288.
(44) Van Doorn, A. R.; Bos, M.; Harkema, S.; Van Eerden, J.; Verboom, W.; Reinhoudt, D. N. *J. Org. Chem.* **1991**, *56*, 2371−2380.
(45) Evans, R. C.; Douglas, P.; Burrow, H. D. *Applied Photochemistry*; Springer: Dordrecht, 2013; p 598.
(46) Guasch, J.; Grisanti, L.; Jung, S.; Morales, D.; D'avino, G.; Souto, M.; Fontrodona, X.; Painelli, A.; Renz, F.; Ratera, I.; Veciana, J. *Chem. Mater.* **2013**, *25*, 808−814.
(47) Gourier, D.; Caurant, D.; Berthet, J. C.; Boisson, C.; Ephritikhine, M. *Inorg. Chem.* **1997**, *36*, 5931−5936.
(48) Poole Jr., C. P.; Farach, H. A. *Handbook of Electron Spin Resonance*; Springer-Verlag: New York, 1999; Vol. 2, p 660.
(49) Meyer, K.; Mindiola, D. J.; Baker, T. A.; Davis, W. M.; Cummins, C. C. *Angew. Chem., Int. Ed.* **2000**, *39*, 3063−3066.
(50) Enright, D.; Gambarotta, S.; Yap, G. P. A.; Budzelaar, P. H. M. *Angew. Chem., Int. Ed.* **2002**, *41*, 3873−3876.
(51) Scott, J.; Gambarotta, S.; Korobkov, I.; Knijnenburg, Q.; De Bruin, B.; Budzelaar, P. H. M. *J. Am. Chem. Soc.* **2005**, *127*, 17204−17206.
(52) Yu, R. P.; Darmon, J. M.; Milsmann, C.; Margulieux, G. W.; Stieber, S. C. E.; Debeer, S.; Chirik, P. J. *J. Am. Chem. Soc.* **2013**, *135*, 13168−13184.
(53) Bowman, A. C.; Milsmann, C.; Atienza, C. C. H.; Lobkovsky, E.; Wieghardt, K.; Chirik, P. J. *J. Am. Chem. Soc.* **2010**, *132*, 1676−1684.
(54) Launer, P. J. *Silicone Compounds Register and Review*; Petrarch Systems: Bristol, PA, 1987; pp 100−103.
(55) Fortier, S.; Kaltsoyannis, N.; Wu, G.; Hayton, T. W. *J. Am. Chem. Soc.* **2011**, *133*, 14224−14227.
(56) Brown, J. L.; Mokhtarzadeh, C. C.; Lever, J. M.; Wu, G.; Hayton, T. W. *Inorg. Chem.* **2011**, *50*, 5105−5112.
(57) Mueller, T. J.; Ziller, J. W.; Evans, W. J. *Dalton Trans.* **2010**, *39*, 6767−6773.
(58) Mueller, T. J.; Fieser, M. E.; Ziller, J. W.; Evans, W. J. *Chem. Sci.* **2011**, *2*, 1992−1996.
(59) Evans, W. J.; Kozimor, S. A.; Ziller, J. W. *Chem. Commun.* **2005**, 4681−4683.
(60) Takase, M. K.; Ziller, J. W.; Evans, W. J. *Chem. - Eur. J.* **2011**, *17*, 4871−4878.

DOI: 10.1021/jacs.5b06217
J. Am. Chem. Soc. 2015, 137, 11115−11125